AUTOREGULATION IN A SIMULATOR-BASED EDUCATIONAL MODEL OF INTRACRANIAL PHYSIOLOGY

W. James Thoman, MS, Dietrich Gravenstein, MD, Jan van der Aa, PhD, Samsun Lampotang, PhD

Thoman WJ, Gravenstein D, Van der Aa J, Lampotang S. Autoregulation in a simulator-based educational model of intracranial physiology.

J Clin Monit 1999; 15: 481–491

ABSTRACT. Objective. To implement a realistic autoregulation mechanism to enhance an existing educational brain model that displays in real-time the cerebral metabolic rate ($CMRO_2$), cerebral blood flow (CBF), cerebral blood volume (CBV), intracranial pressure (ICP), and cerebral perfusion pressure (CPP). **Methods.** A dynamic cerebrovascular resistance (CVR) feedback loop adjusts automatically to maintain CBF within a range of the CPP and defines autoregulation. The model obtains physiologic parameters from a full-scale patient simulator. We assumed that oxygen demand and arterial partial pressure of carbon dioxide (CO_2 responsivity) are the two major factors involved in determining CBF. In addition, our brain model increases oxygen extraction up to 70% once CBF becomes insufficient to support $CMRO_2$. The model was validated against data from the literature. **Results.** The model's response varied less than 9% from the literature data. Similarly, based on correlation coefficients between the brain model and experimental data, a good fit was obtained for curves describing the relationship between CBF and $PaCO_2$ at a mean arterial blood pressure of 150 mm Hg (R^2 = 0.92) and 100 mm Hg (R^2 = 0.70). **Discussion.** The autoregulated brain model, with incorporated CO_2 responsivity and a variable oxygen extraction, automatically produces changes in CVR, CBF, CBV, and ICP consistent with literature reports, when run concurrently with a METI full-scale patient simulator (Medical Education Technologies, Inc., Sarasota, Florida). Once the model is enhanced to include herniation, vasospasm, and drug effects, its utility will be expanded beyond demonstrating only basic neuroanesthesia concepts.

KEY WORDS. Cerebral blood flow, cerebral vascular resistance, cerebral perfusion pressure, $PaCO_2$, PaO_2, cerebral metabolic rate of oxygen consumption, educational model, simulation.

INTRODUCTION

Cerebral blood flow can be influenced by adjusting physiologic variables such as cerebral metabolic rate of oxygen consumption ($CMRO_2$), arterial partial pressure of oxygen (PaO_2), arterial partial pressure of carbon dioxide ($PaCO_2$), and mean arterial blood pressure (MABP). The conceptual basis underlying a clinician's treatment strategy is derived from research on animals and humans, where, generally, only one variable is varied at a time while keeping others constant [1–3].

The goal of this project was to implement a mechanism for autoregulation into an existing brain model [4] and generate a dynamic display of intracranial variables such as intracranial pressure (ICP), cerebral blood flow (CBF), and cerebral blood volume (CBV) as they simultaneously change and affect each other. When

From the Department of Anesthesiology, University of Florida College of Medicine; the Departments of Electrical and Computer Engineering, Mechanical Engineering, and Engineering Science, University of Florida College of Engineering; the University of Florida Brain Institute; and Shands Hospital at the University of Florida, Gainesville, Florida, U.S.A.

Received Jul 6, 1999, and in revised form Nov 11, 1999. Accepted for publication Nov 22, 1999.

Address correspondence to Samsun Lampotang, PhD, Department of Anesthesiology, University of Florida College of Medicine, PO Box 100254, Gainesville, FL 32610-0254, U.S.A.
E-mail: sem@anest4.anest.ufl.edu

Journal of Clinical Monitoring and Computing **15**: 481–491, 1999.

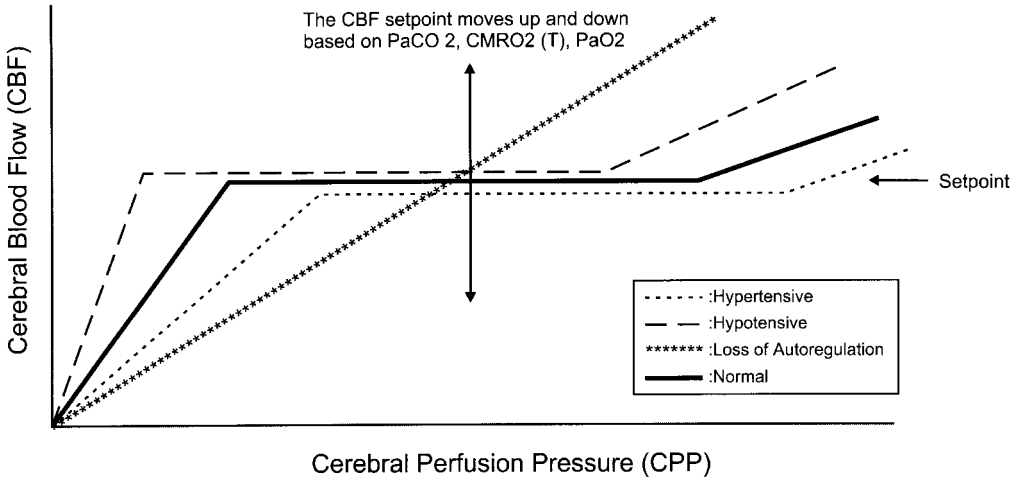

Fig. 1. The relationship between cerebral blood flow (CBF) and cerebral perfusion pressure (CPP) in an autoregulated brain model. The slope of the line at both ends of autoregulation represents the conductance or the inverse of resistance of the cerebral vasculature. By setting two extreme values of resistance, the autoregulation zone (horizontal portion) can be customized to model patients with various degrees of loss of autoregulation.

integrated to a full-scale patient simulator (Human Patient Simulator v. B, Medical Education Technologies, Inc., Sarasota, FL) [5], the brain model with autoregulation features provides a real-time window into events within the intracranial space and may become a new educational tool for learning the management of intracranial dynamics. It should be emphasized that the goal of the model is to be an educational tool, incorporating many simplifying assumptions, not necessarily a highly accurate physiologic model for precisely predicting patient response.

Autoregulation was modeled by designing a dynamic cerebrovascular resistance (CVR) system. In addition to CPP and oxygen demand/delivery balance, the effect of $PaCO_2$ (i.e., CO_2 responsivity) is an independent controlling factor of CBF. Based on these factors, CVR is calculated in the model to automatically adjust to maintain CBF at a set point within the autoregulation zone. We describe the implementation of the model and its validation against responses described in the literature.

METHODS

Description of the model

Similar to our first model of intracranial physiology [4], the brain model described here is composed of four separate volumes: brain tissue, blood, cerebrospinal fluid, and a "mass." Under normal physiologic conditions, the sum of these volumes equals the cranial cavity volume (1300 ml) and the "mass" volume is zero. The elastance relationship described in our first model [4] is used to determine ICP.

Autoregulation functions to maintain a constant CBF when the cerebral perfusion pressure (CPP) varies within the 50–150 mm Hg range (Figure 1) [1] by modulating CVR. It also plays an important role in ensuring that adequate oxygen is delivered to brain tissues. $PaCO_2$, independently of CPP and PaO_2, also affects CVR [6–9]. Thus, autoregulation requires that changes in oxygen demand produce corresponding changes in oxygen delivery. The mechanisms by which oxygen delivery can be changed include changes in hemoglobin concentration ([Hb]), CBF (through CVR), 2,3-diphosphoglycerate concentration ([DPG]) and arterial oxygen saturation (SaO_2). Physiologically, [Hb], [DPG] and oxygen saturation cannot be quickly altered to meet changes in demand. Therefore, we assume that the mechanism of autoregulation that regulates CBF during ischemia also occurs through the modulation of CVR. In our model, CVR modulation is the principal mechanism for satisfying oxygen demand.

Autoregulation, using the relationship between CVR and CBF, is described by Equation (1), where CPP is obtained from Equation (2), "t" represents time, and we assume that a linear resistance can represent the cerebral vasculature. From Equation (1), it can be seen that under constant CPP, CBF is

$$\mathrm{CBF}(t) = \frac{\mathrm{CPP}}{\mathrm{CVR}(t)} \tag{1}$$

inversely proportional to CVR. A decrease in CVR will increase CBF and vice-versa. Because CBF determines the amount of oxygen supplied (SaO_2 and [Hb] remaining constant), the controlling factor that affects CVR and, thus, CBF is oxygen demand, which is based on the cerebral metabolic rate.

CPP is defined as the mean arterial blood pressure (MABP) minus either ICP or central venous pressure (CVP), whichever is greater. This model uses ICP because its default value of 12 mm Hg is greater than the normal CVP range of 0 to 6 mm Hg. A common clinical objective is to maintain CPP above the lower limit of 50 mm Hg, which represents the lowest CPP value on the autoregulation zone (horizontal portion) of Figure 1 [1]. The CPP is calculated using Equation (2) as follows:

$$\mathrm{CPP} = \mathrm{MABP} - \mathrm{ICP\ (or\ CVP)} \tag{2}$$

The oxygen demand is equal to $CMRO_2$, which is influenced by anesthetic agents, temperature, and seizures, among other things. Therefore, in modeling autoregulation, the oxygen demand rate is based directly on the metabolic rate and is used to determine the set point CBF for oxygen. Equation (3) [4, 10, 11] defines $CMRO_2$ solely as a function of temperature [4]. For a normal body temperature of 37 °C, under normal circumstances, $CMRO_2$ is 3.56 ml O_2/100 ml brain/min.

$$\mathrm{CMRO_2} = \exp(-2.7579 + 0.1089 * \mathrm{T}) \tag{3}$$

The amount of oxygen delivered to the brain is determined by arterial oxygen content (CaO_2; function of [Hb], SaO_2, and PaO_2) and CBF (function of CPP and CVR). CaO_2 is determined using Equation (4) [12] where the constant 0.0031 represents the amount of oxygen that dissolves in blood without binding to hemoglobin.

$$\mathrm{CaO_2} = \mathrm{SaO_2}\,([\mathrm{Hb}] * 1.39) + \mathrm{PaO_2}\,(0.0031) \tag{4}$$

SaO_2 is determined from PaO_2 using a standard oxygen-hemoglobin dissociation curve [13]. The shifting of the dissociation curve by factors such as temperature, [DPG] and pH is not modeled. The dissociation curve was broken into three segments, to get the best possible curve fitting (Origin, Microcal, Northampton, MA). Equations (5), (6) and (7) represent SaO_2 as a function of PaO_2 and are embedded in our brain model. (Units: SaO_2 (%) and PaO_2 (mm Hg))

1. for $0 \le \mathrm{PaO_2} < 40$

$$\begin{aligned}\mathrm{SaO_2} = {} & -0.9175607 + 1.0438527 \cdot \mathrm{PaO_2} \\ & + 0.021241344 \cdot (\mathrm{PaO_2})^2\end{aligned} \tag{5}$$

2. for $40 \le \mathrm{PaO_2} < 140$

$$\begin{aligned}\mathrm{SaO_2} = {} & -34.991452 + 4.766072 \cdot \mathrm{PaO_2} \\ & - 0.067696104 \cdot (\mathrm{PaO_2})^2 \\ & + 0.0004358606 \cdot (\mathrm{PaO_2})^3 \\ & - 1.045397\mathrm{E} - 6 \cdot (\mathrm{PaO_2})^4\end{aligned} \tag{6}$$

3. for $\mathrm{PaO_2} \ge 140$

$$\mathrm{SaO_2} = 100\% \tag{7}$$

Under normal conditions, the amount of oxygen delivered to the brain far exceeds the demand. When CBF decreases below the lower limit of autoregulation but the oxygen demand remains high, extraction of oxygen from blood can be increased [14]. For our model, the default oxygen extraction was calculated to be 31% in the autoregulation zone, using the default values for CBF (52.5 ml/100 g brain/min), CaO_2 (21 ml/100 ml blood) [12], and $CMRO_2$ (3.56 ml O_2/100 ml brain/min) in Equation (8) and solving for the oxygen extraction (ext). As the lower limit of the autoregulation zone is reached (left side of flat portion), CBF starts to decrease linearly with CPP. At this point, the oxygen extraction starts to increase in order to meet the oxygen demand. If CPP falls below where the oxygen extraction has been maximized at 70%, ischemia occurs [15]. The set point for the fraction of CBF governed by oxygen, CBF_{sp,O_2}, is determined by using PaO_2 (indirectly via Equation (4)) and $CMRO_2$ in Equation (8). "Set point" describes the CBF required to meet $CMRO_2$. CaO_2 is determined using Equation (4).

$$\mathrm{CBF_{sp,O_2}} = \frac{\mathrm{CMRO_2}}{\mathrm{CaO_2} * \mathrm{ext}} \tag{8}$$

Similarly, the set point for the fraction of CBF influenced by carbon dioxide, CBF_{sp,CO_2}, defines CBF based on $PaCO_2$. Using previously obtained equations [4], the percentage value of CBF (%CBF) is calculated based on $PaCO_2$. The CBF_{sp,CO_2} is converted from %CBF value to actual CBF using Equation (9).

$$\mathrm{CBF_{sp,CO_2}} = \frac{52.5 * \%\mathrm{CBF}}{100\%} \tag{9}$$

where 52.5 ml/100 g brain/min is the default CBF.

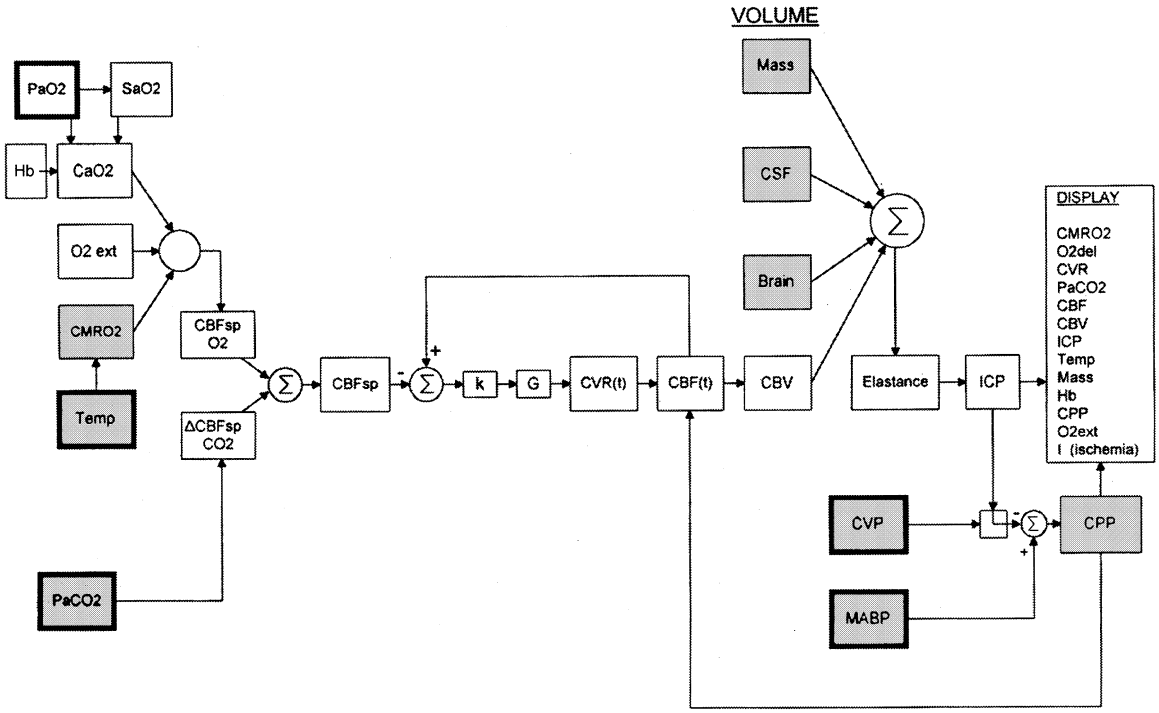

Fig. 2. Flow chart of brain model with autoregulation. Highlighted boxes represent the original brain model and boxes surrounded by bold lines represent input data from the full-scale human patient simulator.

Both the PaO_2 and $PaCO_2$ set points cause the autoregulation zone (Figure 1) to move up and down based on oxygen demand and $PaCO_2$. Therefore, for our model, CBF_{sp,CO_2} is made independent of CBF_{sp,O_2} and an additive relationship is used in Equation (10) for determining the set point CBF (CBF_{sp}). The effect of $PaCO_2$ on CBF ($\Delta CBF_{sp,CO_2}$) is determined by subtracting the default CBF (52.5 ml blood/100 g brain/min) from CBF_{sp,CO_2}. Multiplying CBF_{sp,O_2} with $\Delta CBF_{sp,CO_2}$ to get CBF_{sp} was not an option because CBF_{sp,O_2} would no longer be independent of $\Delta CBF_{sp,CO_2}$ in its effect on CBF_{sp} when $\Delta CBF_{sp,CO_2}$ is zero.

$$CBF_{sp} = CBF_{sp,O_2} + \Delta CBF_{sp,CO_2} \tag{10}$$

CBF_{sp} is determined using PaO_2, $PaCO_2$, and $CMRO_2$ (Figure 2). Varying these physiologic parameters shifts CBF_{sp} up or down. The CPP range of the autoregulation zone is set by a lower and upper limit of CVR. The limits of CVR at both extremes of the autoregulation zone define the inverse of the slopes on a CBF versus CPP graph. The multiple autoregulation curves in Figure 1 illustrate the capability of the model to adjust for cases of hypertension, hypotension and loss of autoregulation. In the latter case, the autoregulation curve is represented by a single line passing through the origin with no flat portion (Figure 1).

Using the relationship between oxygen demand and CBF, a dynamic feedback system was implemented (Figure 2). The feedback system models autoregulation via CVR modulation. Within the autoregulation zone, CBF and CVR will continuously adjust so that the oxygen supplied will meet the demand set by the brain at the lowest (default) extraction rate.

In the feedback loop, CVR is adjusted so that the actual CBF, CBF(t), matches CBF_{sp}. For example, if $CMRO_2$ goes up, the resultant increase in CBF_{sp} will cause a difference between CBF_{sp} and the CBF at "t" minus one second, CBF(t − 1). In the feedback loop, CVR will decrease so that CBF(t) can increase to match CBF_{sp}. Equation (11) is used to determine the new resistance CVR(t) based on the previous resistance CVR(t − 1) and the "error" in CBF. The change in CVR is determined by multiplying the difference between the previous flow CBF(t − 1) and the CBF_{sp} by a gain G and a sensitivity constant k set to unity. The dimensionless constant "k" allows the user to change the sensitivity of the CVR response without changing the gain. With "k" set to unity and maintaining a constant MABP and ICP, the gain was determined by trying to match CBF(t) to CBF_{sp}(t) within one time

step, Δt (1 sec). Starting with both CBF(t) and CBF(t − 1) at default values of 52.5 ml/100 g brain/min, an average MABP of 75 mm Hg and an ICP of 12 mm Hg, the default CVR(t) and CVR(t − 1) were determined, using Equation (1), to be 1.22 mm Hg/(ml/100 g brain/min). Using the default CVR values and default CBF(t − 1), the gain was determined by keeping MABP, ICP, $CMRO_2$ and PaO_2 fixed at their default values and varying the $PaCO_2$ in 2 mm Hg increments. $PaCO_2$ was chosen as the tuning variable because the CBF vs. $PaCO_2$ plot has a constant slope over a clinically relevant $PaCO_2$ range such that a single given G can be used for the entire $PaCO_2$ range of 20–80 mm Hg (see Figure 4). Secondly, the response of CVR to changes in $PaCO_2$ is fast, due to the rapid diffusion of CO_2 across the blood-brain barrier [6]. Also, the bicarbonate buffer system [13] in humans limits the magnitude of $\Delta PaCO_2$ over Δt. The fast response and the fact that $\Delta PaCO_2$ is small over Δt justify our assumption that CVR will change over 1 sec in order to achieve the desired CBF. Because $PaCO_2$ was the only changing variable, we could determine CBF_{sp} based on $PaCO_2$ and calculate the CVR(t) (Equation (1)), which would cause CBF(t) to equal CBF_{sp}. Solving equation 11, G was determined to be 0.021239 mm Hg/(ml/100 g brain/min) [1].

$$\begin{aligned} &CVR(t) = \\ &\quad CVR(t-1) + k * G * [CBF(t-1) - CBF_{sp}(t)] \end{aligned} \tag{11}$$

The blood volume of the brain model (Equation (12)) is incremented by dividing CBF(t) by 60 (60 sec/min) and multiplying by a factor of 13 (1300 g total brain divided by usual denominator unit of 100 g brain) in order to get the total volume of blood entering the entire brain every second. Similarly, the total blood volume leaving the entire brain every second, CBF_{out}, is subtracted from the blood-brain volume. In Equation (12), the cerebral blood volume CBV(t) is updated every tenth of a second ($\Delta t = 0.1$ sec).

$$CBV(t) = CBV(t-1) + \frac{13}{60}\,(CBF(t) - CBF_{out})\Delta t \tag{12}$$

A literature search did not produce the quantitative data required to model the out-flow mechanism for the brain. Consequently, a linear relationship between CBV and CBF adapted from Leenders et al. [3] (Equation (13)) is used to set limits to CBV; the model sets an upper or a lower limit blood volume, CBV_{limit} that is derived from CBF(t) and Equation (13) [4]. The number 10.23476 represents the inverse of the slope for our regression line through Leenders' data. Units: CBV_{limit} (ml/100 g brain), CBF (ml/100 g brain/min)

$$CBV_{limit}(t) = \frac{13 * CBF(t)}{10.23476} \tag{13}$$

$CBV_{limit}(t)$ is set according to CBF(t) and changes continuously as CBF(t) is updated. When CBV(t) (Equation (12)) matches $CBV_{limit}(t)$ (Equation (13)), the out-flow rate (CBF_{out}) is set equal to the in-flow rate (CBF(t)), which allows CBV(t) to remain constant. For example, in a normal patient with a CBV(t) of 75 ml and all the parameters set to their default values, CBF_{out} is set equal to the CBF(t) default value of 52.5 ml blood/100 g brain/min. While the patient remains hemodynamically stable, CBF(t), CBF_{out}, and CBV(t) will remain constant at their default values. If flow demand increases, CBF(t) will start to increase while the out-flow rate remains constant at the original setting (52.5 ml blood/100 g brain/min, for this example). In this case, assume that CBF(t) was increased to 65 ml blood/100 g brain/min. According to Equation (12), CBV(t) will start to increase from its default value. The blood volume will increase until CBV(t) equals $CBV_{limit}(t)$, which is determined by CBF(t) (Equation (13)). In this example, CBF(t) is 65 ml blood/100 g brain/min and $CBV_{limit}(t)$ is calculated to be 95 ml. Once CBV(t) is equal to $CBV_{limit}(t) \pm 4$ ml, CBF_{out} is set equal to CBF(t) and the intracranial blood volume will remain at CBV_{limit} (95 ml) until CBF(t) changes once more. Similarly if flow demand decreases, the in-flow rate will start to decrease while the out-flow rate will remain unchanged. Because the in-flow rate is smaller than the out-flow rate, CBV(t) will decrease until it matches the CBV_{limit} corresponding to the lower CBF(t), within ± 4 ml.

The complete flow chart for the brain model incorporating autoregulation is shown in Figure 2. CBF is calculated using Equation (1) and the flow chart shows the input from CPP and CVR onto the CBF(t) box. The dynamic feedback loop is the one going from the CBF(t) box to the operator circle. In this loop, CBF(t) is driven towards CBF_{sp} by varying CVR according to the "error" in CBF.

Validation techniques

Model validation consisted of three parts. First, the model's output was compared to a set of standardized, idealized curves that describe the relationship among CPP, CBF, $PaCO_2$, PaO_2, as published by Michenfelder [1]. For convenience, these curves will henceforth be cited as Michenfelder's curves. Second, the model's output was compared to experimental data from Harper and Glass [16]. Finally, the model was evaluated for

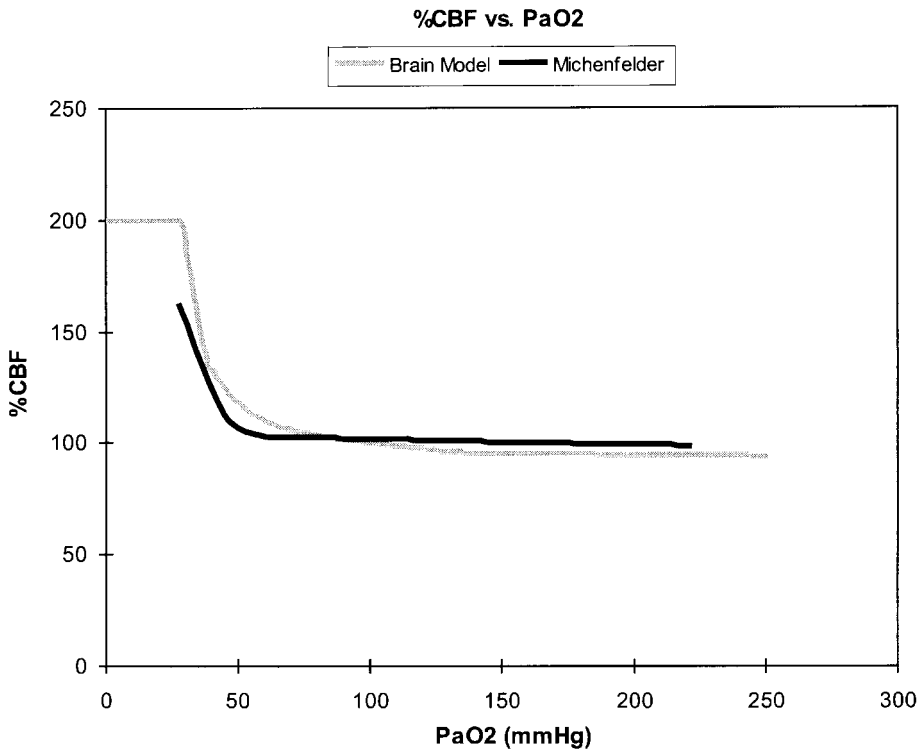

Fig. 3. The relationship between cerebral blood flow (CBF) and arterial partial pressure of oxygen (PaO_2) generated by the brain model (gray) compared to the Michenfelder curve (black). Arterial partial pressure of carbon dioxide ($PaCO_2$) and mean arterial blood pressure (MABP) held constant at 40 and 75 mm Hg, respectively.

clinical realism (plausible time course and magnitude of changes) in the Human Patient Simulator. To validate the model, we reproduced some of the experiments conducted by Michenfelder [1]. All physiologic input variables were set to their default values and kept constant while only the input variable of interest was changed. The input variables to the brain model are PaO_2, $PaCO_2$, MABP, temperature, [Hb], CVR range (autoregulation) and a "mass" volume (Figure 2). In order to compare the response of the brain model to Michenfelder's curves, temperature (36.5 °C), [Hb] (15 gm/dL), CVR range (normal: 0.6–3.0 mm Hg/ml/100 g brain/min), and mass volume (0 ml) were set to their normal default values, defining a normal brain. The remaining three variables PaO_2, $PaCO_2$, and MABP or CPP were each tested independently while the other two variables were set to their default values (PaO_2 = 100 mm Hg, $PaCO_2$ = 40 mm Hg, and MABP = 75 mm Hg). During the test, CVR, CBF, and CBV are dynamically changing in response to changes in PaO_2, $PaCO_2$, or MABP. The %CBF is plotted as a function of PaO_2, $PaCO_2$, and CPP and compared to Michenfelder's curves.

In order to compare Michenfelder's curves to the model-generated curves, we divided the absolute error (%CBF) between the two corresponding curves by the %CBF value reported by Michenfelder's curve, for each 1 mm Hg increment along the X-axis. The summation of the absolute, normalized errors was then divided by the number of points along the X-axis and multiplied by 100% in order to get a percent value, E, for deviation of the model curve in comparison to Michenfelder's curve (Equation (14)).

$$E = \frac{\sum_{i=0}^{i=n} \frac{|Y_{Mi} - Y_{BMi}|}{Y_{Mi}}}{n} * 100\% \qquad (14)$$

M = Michenfelder data, BM = brain model data, Y = %CBF, i = data points along X-axis

RESULTS

The error between Michenfelder's curve and our model for the relationship between %CBF and PaO_2 is 5.24% (Figure 3). PaO_2 and CVR were initialized to 0 mm Hg and 0.6 mm Hg/ml/100 g brain/min respectively. PaO_2

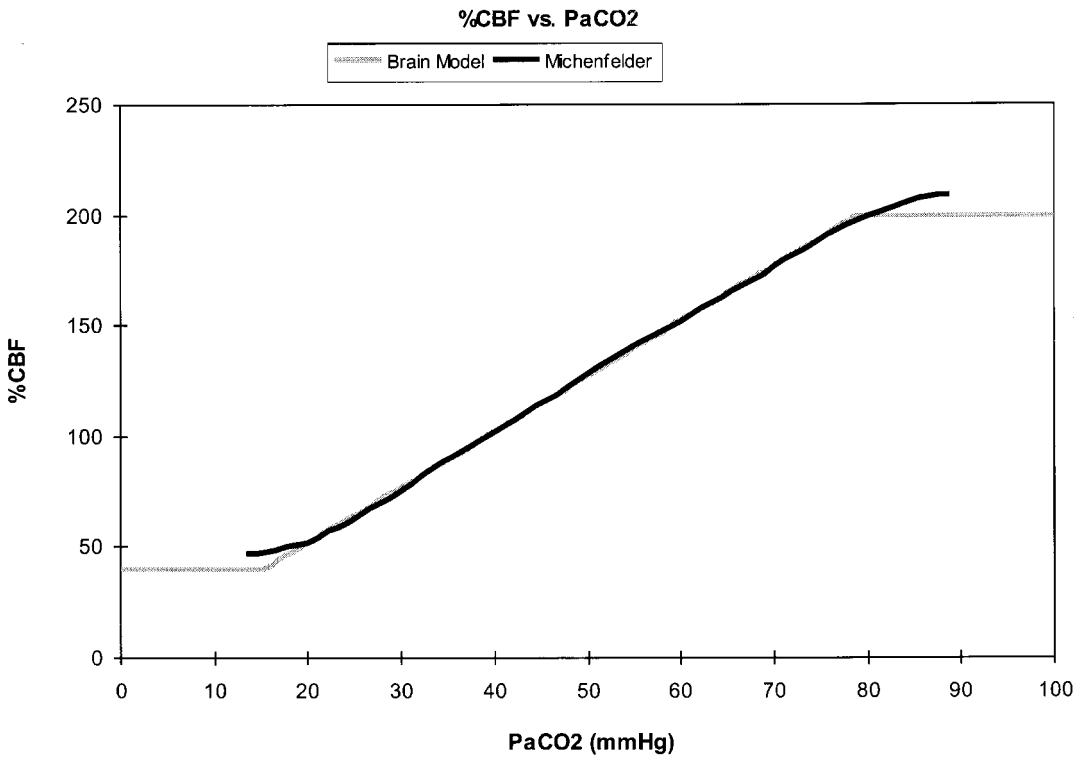

Fig. 4. The relationship between cerebral blood flow (CBF) and arterial partial pressure of carbon dioxide ($PaCO_2$) generated by the brain model (gray) compared to the Michenfelder curve (black). Arterial partial pressure of oxygen (PaO_2) and mean arterial blood pressure (MABP) held constant at 100 and 75 mm Hg, respectively.

was increased incrementally by 1 mm Hg every second while CVR was allowed to adjust itself based on the autoregulation mechanism. Initially, below a PaO_2 of 30 mm Hg, the flat portion of the curve represents a vascular system that is maximally dilated (lower end of autoregulation) in order to maximize oxygen delivery by maximizing CBF. Once PaO_2 exceeds 30 mm Hg, CaO_2 is sufficient and autoregulation starts decreasing CBF by increasing CVR. As the PaO_2 and blood oxygen saturation (SaO_2) increase, the increased CaO_2 results in further decreases in CBF. The curve finally flattens out because SaO_2 becomes maximized.

The brain model uses equations [4] derived from Michenfelder for determining the %CBF based on $PaCO_2$. To generate output, all variables were set to their default values except for $PaCO_2$ and CVR, which were set to their initial values of 0 mm Hg and 3.0 mm Hg/ml/100 g brain/min. $PaCO_2$ was increased incrementally by 1 mm Hg every second while CVR was allowed to adjust itself. Similar to the Michenfelder curve, the curve generated by the brain model flattens out at both ends of the $PaCO_2$ spectrum (Figure 4). The curve flattens out because the lower and upper limits of autoregulation are reached. As the $PaCO_2$ decreases, the cerebral vasculature continues to constrict in order to reduce blood flow. Once the vasculature has reached its limit and cannot constrict any more, blood flow becomes solely a function of blood pressure. As long as the blood pressure is constant, as enforced here, the blood flow will remain constant. Similarly at the upper limits of autoregulation, the vasculature can no longer dilate, causing a constant blood flow under constant pressure. The small error of 2% reflects the good fit between the model's output and Michenfelder's curve.

Figure 5 shows the autoregulation curve that describes the relationship between %CBF and CPP. For the brain model, normal autoregulation is set with a minimum CVR of 0.6 mm Hg/ml/100 g brain/min and a maximum CVR of 3.0 mm Hg/ml/100 g brain/min. The inverse of the lower and upper CVR values represents the slopes of the gray lines shown at both extremes of autoregulation in Figure 5. To generate the curve, all variables were set to their default values. CVR was initialized to 0.6 mm Hg/ml/100 g brain/min and MABP was initialized to 12 mm Hg to ensure that the CPP started at 0 mm Hg because the CPP is determined by subtracting the ICP (default value 12 mm Hg) from the MABP. The MABP was then in-

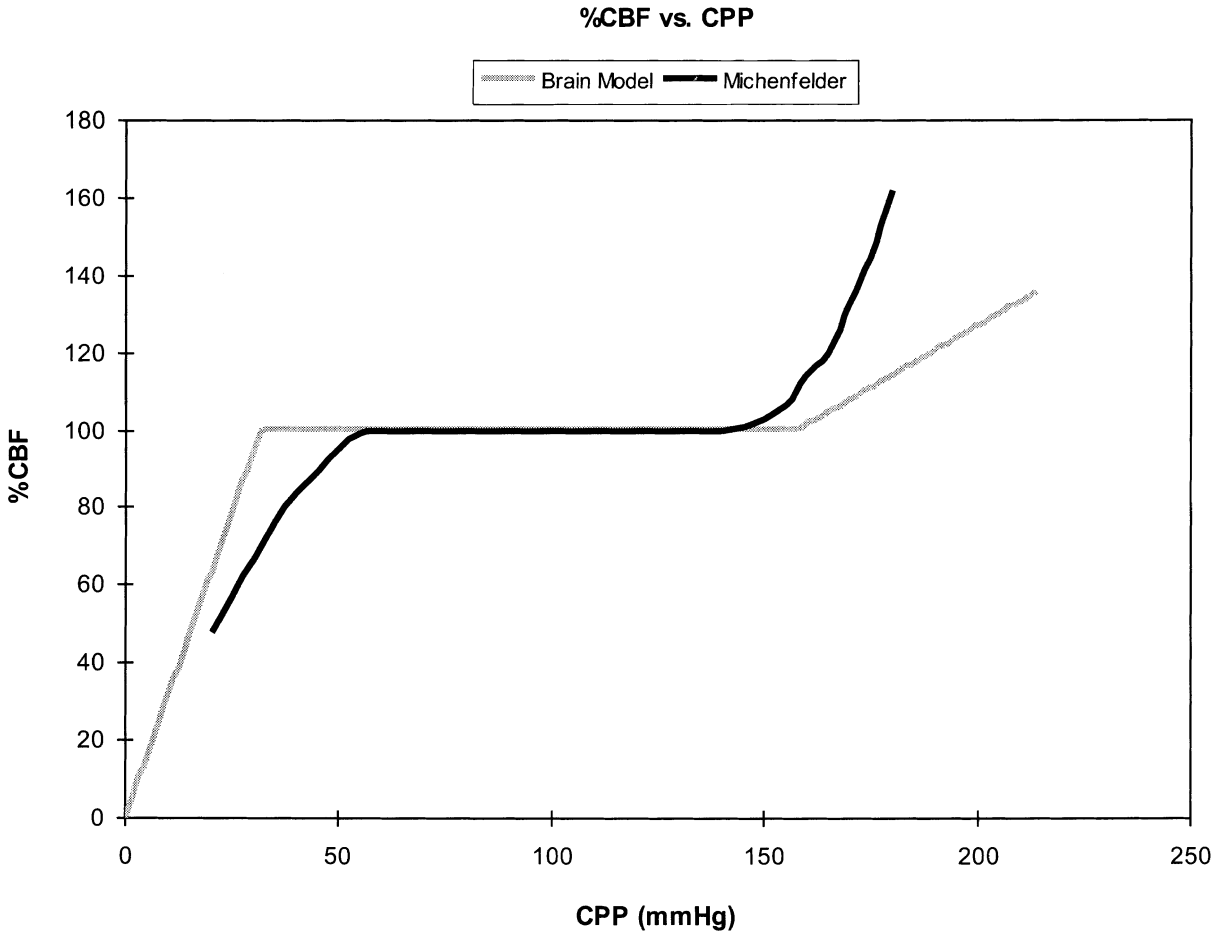

Fig. 5. The relationship between cerebral blood flow (CBF) and cerebral perfusion pressure (CPP) generated by the brain model (gray) compared to the Michenfelder curve (black). Arterial partial pressure of oxygen (PaO_2) and arterial partial pressure of carbon dioxide ($PaCO_2$) held constant at 100 and 40 mm Hg, respectively.

creased incrementally by 1 mm Hg every second until it reached 220 mm Hg. CVR was allowed to adjust itself throughout the run. The error between the two curves in Figure 5 is 8.37%. The model-generated curve varies from the Michenfelder curve at both the lower and upper end of autoregulation, causing the larger error value.

The ability to customize autoregulation at the beginning of each simulation enhances the flexibility of the brain model as a learning tool allowing simulation of a variety of cases as shown in Figure 1. We reproduced curves experimentally obtained by Harper and Glass [16] by changing the CVR limits of autoregulation until a good visual fit was obtained. Harper and Glass studied the effects of $PaCO_2$ on CBF at MABPs of 150, 100, and 50 mm Hg in dogs (Figure 6). Because Harper and Glass did not give R^2 values for their data, the coordinates of their data [16] were manually measured and entered into a Microsoft Excel spreadsheet so that the R^2 values could be compared. An exponential curve fit was done for the 50 mm Hg blood pressure data, while a third order polynomial curve fit was performed for the 100 and 150 mm Hg blood pressure data. Figure 6 shows the %CBF response to $PaCO_2$ in normotensive animals (MABP = 150 mm Hg) where 100% CBF represents normal blood flow at a $PaCO_2$ value of 40 mm Hg. The curve generated by the brain model (gray) correlates very well ($R^2 = 0.92$) with the experimental data for normotensive animals. The black curve represents our curve fit of Harper's data ($R^2 = 0.93$). In the hypotensive animals with a MABP of 100 mm Hg (Figure 6), the brain model provides a steeper response to $PaCO_2$ within the autoregulation limits than the curve fit data, and the brain model's response (gray) is within the data range recorded by Harper and Glass ($R^2 = 0.70$ for brain model, $R^2 = 0.78$ for Harper and

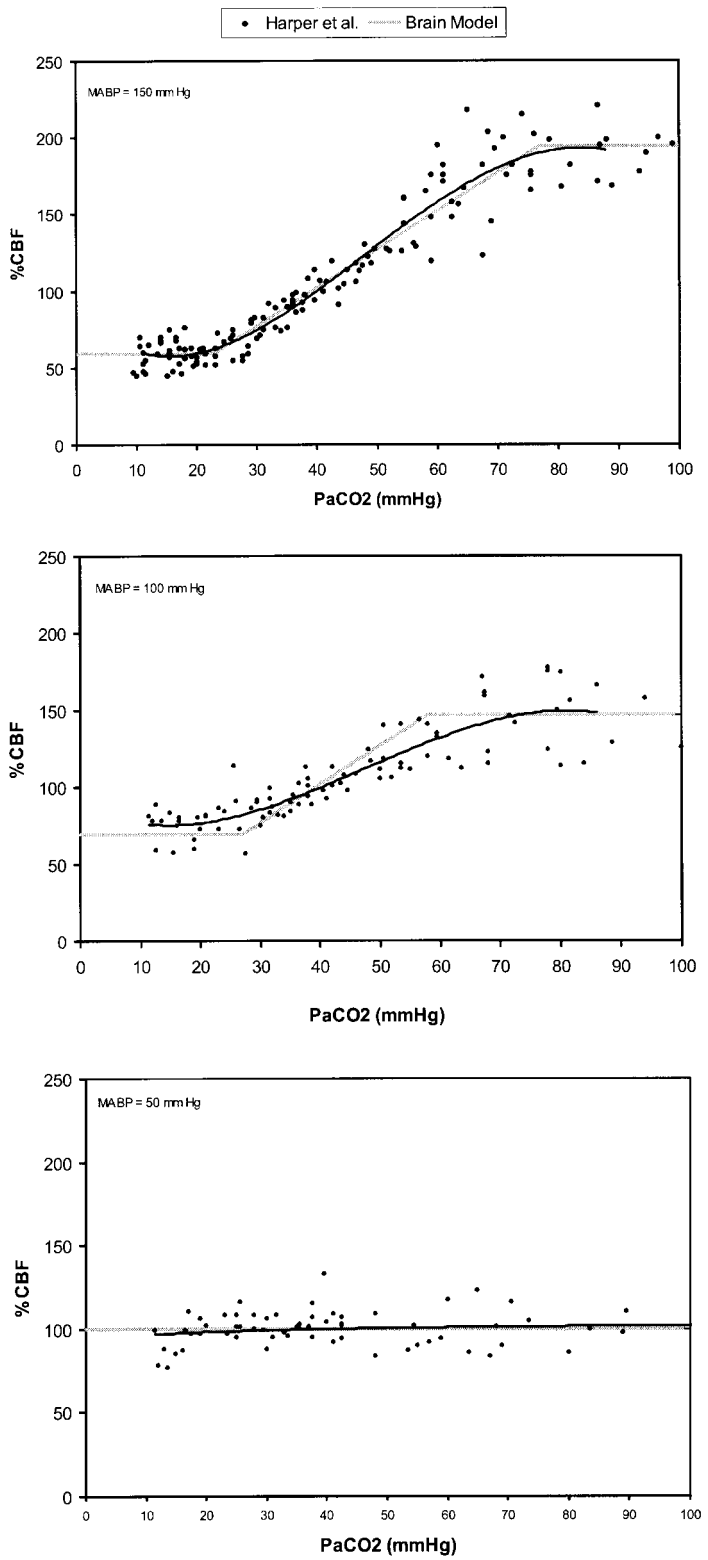

Fig. 6. The effects of arterial partial pressure of carbon dioxide ($PaCO_2$) on cerebral blood flow (CBF) in normotensive animals at a mean arterial blood pressure (MABP) of 150 mm Hg and hypotensive animals at a MABP of 100 and 50 mm Hg. A cerebral blood flow (CBF) of 100% represents normal blood flow value for an arterial partial pressure of carbon dioxide ($PaCO_2$) of 40 mm Hg.

Glass). Finally the effects of $PaCO_2$ on CBF at a MABP of 50 mm Hg can also be seen in Figure 6. Visually, the brain model's response (gray) is close to the curve fit (black) of Harper and Glass's data. The model's low R^2 value (0.0014) is explained by the large variance of the experimental data collected (R^2 = 0.0165 for Harper and Glass's data).

During clinical evaluation in a simulated environment, in several scenarios, ICP increased with laryngoscopy from about 15 mm Hg to 38 mm Hg over about 30 seconds. The magnitude and response time of the change of ICP for the brain model are within the range (ICP peaking at 24–44 mm Hg after 25–63 s following laryngoscopy) reported by Burney and Winn [17] starting with an ICP of approximately 15 mm Hg.

DISCUSSION

The work to build an autoregulated brain simulator for teaching and research has been underway for many years [18, 19]. The brain model presented here differs from these earlier efforts in that it is linked to a human patient simulator that provides the model with physiologic parameters like $PaCO_2$, MABP, CVP, temperature and SaO_2. The clinician interacts with the simulator, not a computer, to give pharmacologic, ventilatory and hemodynamic support. The brain model, in turn, responds in real time to these interventions and displays their effects on the brain.

Because experiments where multiple variables are changing simultaneously are, by definition, uncontrolled experiments, there were no such experiments in the literature that we could use to validate our model. In effect, the third step of the validation, clinical evaluation attempts to assess the behavior of the model while multiple variables are changing simultaneously. The model described here may facilitate providing benchmark experiments where multiple variables change simultaneously.

Clinicians are conventionally taught intracranial pressure management using idealized depictions of intracranial dynamics, such as Michenfelder's curves. Therefore, it was essential that the model match these relationships [1] and the descriptive models commonly used by clinicians who are educators in this area. Although the validity of these curves has been questioned [20], the prevailing thought, as represented in clinical text books, is consistent with our model. The similar results obtained suggest that the dynamic autoregulation mechanism we implemented was appropriate.

One limitation of the brain model can be seen at both the lower and upper end of the autoregulatory curve in Figure 5. The brain model shows a constant resistance at both ends (straight lines passing through the origin) while Michenfelder's curve shows changing resistance at both ends (curves not passing through the origin). Based on fluid dynamics, we would anticipate a fixed resistance as shown by the brain model. However, the physiology of the intracranial vessels allows for partially collapsed vessels at very low perfusion pressures causing the CVR to increase slightly. Similarly, at extremely high perfusion pressures, passive vascular dilation results in a slight decrease in CVR causing the autoregulatory curve to become steeper [6].

Another assumption that limits the model is Equation (2), CPP = MABP – ICP (or CVP). This is a valid relationship in a static analysis but may not be so in a dynamic one. Relatively poor correlation exists between short to moderate duration increases in CVP and ICP [21]. We elected to use Equation (2), however, because other methods of calculating CPP would have required numerous assumptions.

This version of the brain model lacks any direct response to drugs. Thus, influences of inhalational anesthetics and other drugs, such as vasoconstrictors, vasodilators, uncoupling of $CMRO_2$ from CBF, and decreasing $CMRO_2$ can not yet be demonstrated. These limitations of the model, however, are not crippling. The autoregulated brain model, when used with a patient simulator, with incorporated CO_2 responsivity and a variable oxygen extraction, automatically produces changes in CVR, CBF, CBV, and ICP consistent with those reported in the literature and textbooks. It can therefore be used to teach basic neuroanesthesia concepts by allowing trainees to see inside the brain and evaluate the results of their actions in real time. Future development of the brain model, which includes incorporating the effects of drugs on brain perfusion and metabolism, and modeling of special situations, such as herniation and vasospasm, should enhance its utility.

We would like to thank Drs. N. Gravenstein, Luttge, J.S. Gravenstein, Good, Mahla, Cucchiara, Black, Morey, Sulek, Faberowski, and Van Meurs for their support and expertise in developing the brain model. We would also like to thank Dr. van Oostrom for providing us with a graphical plotting routine, and Michael Ellis for his help with the communication protocols of the HPS simulation, Anita Yeager for editorial assistance and Kendra Kuck for the graphics. Finally, we would like to thank Dr. Beneken for sharing his expertise in modeling physiology.

This work was supported in part by a grant from the I. Heermann Anesthesia Foundation.

REFERENCES

1. Michenfelder JD. Anesthesia and the Brain. New York: Churchill Livingstone, 1988: 3–21
2. Sulek C. Intracranial pressure. In: Black S, Cucchiara RF, Michenfelder JD, eds. Clinical neuroanesthesia, 2nd ed. New York: Churchill Livingstone, 1998: 73–123
3. Leenders L, Perani D, Lammertsma AA, Heather JD, Buckingham P, Healy MJR, Gibbs JM, Wise RJS, Hatazawa J, Herold S, Beaney RP, Brooks DJ, Spinks T, Rhodes C, Frackowiak RSJ, Jones T. Cerebral blood flow, blood volume and oxygen consumption. Brain 1990; 113: 27–47
4. Thoman WJ, Lampotang S, Gravenstein D, van der Aa J. A computer model of intracranial dynamics integrated to a full-scale patient simulator. Comput Biomed Res 1998; 31: 32–46
5. Lampotang S, Good ML, van Meurs WL, Caravano RG, Azukas J, Rueger EM, Gravenstein JS. The University of Florida/Loral Human Patient Simulator (abstract). J Anesth 1995; 9: SS1–5
6. Young WL, Ornstein E. Cerebral and spinal cord blood flow. In: Cottrell JE, Smith DS, eds. Anesthesia and neurosurgery. St. Louis, MO: Mosby-Year Book, Inc., 1994: 17–58
7. Jones MD, Traystaman RJ, Simmons MA, Molteni RA. Effects of changes in arterial O_2 content on cerebral blood flow in the lamb. Am J Physiol 1981, 240: H209–H215
8. Drummond JC, Shapiro HM. Cerebral physiology. In: Miller RD, ed. Anesthesia. New York: Churchill Livingstone, 1994: 689–729
9. Ellingsen I, Hauge A, Nicolaysen G, Thoresen M, Walloe L. Changes in human cerebral blood flow due to step changes in PaO_2 and $PaCO_2$. Acta Physiol Scand 1987; 129: 157–163
10. Croughwell N, Smith LR, Quill T, Newman M, Greeley W, Kern F, Lu J, Reves JG. The effect of temperature on cerebral metabolism and blood flow in adults during cardiopulmonary bypass. J Thorac Cardiovasc Surg 1992; 103: 549–554
11. Greeley WJ, Kern FH, Ungerleider RM, Boyd JL, Quill T, Smith LR, Baldwin B, Reves JG, Sabiston DC. The effect of hypothermic cardiopulmonary bypass and total circulatory arrest on cerebral metabolism in neonates, infants, and children. J Thorac Cardiovasc Surg 1991; 101: 783–794
12. Barash PG, Cullen BF, Stoelting RK. Handbook of Clinical Anesthesia. Philadelphia: JB Lippincott Company, 1991: 452
13. Guyton AC, Hall JE. Textbook of Medical Physiology. Philadelphia: WB Saunders Company, 1996: 513–520
14. Fitch W. Cerebral metabolism. In: Cottrell JE, Smith DS, eds. Anesthesia and neurosurgery. St. Louis, MO: Mosby-Year Book, Inc., 1994: 1–16
15. Chan KH, Miller JD, Dearden NM, Andrews PJD, Midgley S. The effects of changes in cerebral perfusion pressure upon middle cerebral artery blood flow velocity and jugular bulb venous oxygen saturation after severe brain injury. J Neurosurg 1992; 77: 55–61
16. Harper AM, Glass HI. Effect of alterations in the arterial carbon dioxide tension on the blood flow through the cerebral cortex at normal and low arterial blood pressures. J Neurol Neurosurg Psychiatry 1965; 28: 449–452
17. Burney RG, Winn R. Increased cerebrospinal fluid pressure during laryngoscopy and intubation for induction of anesthesia. Anesth Analg 1975; 54: 687–690
18. Ursino M, Di Giammarco P. A mathematical model of the relationship between cerebral blood volume and intracranial pressure changes: The generation of plateau waves. Ann Biomed Eng 1991; 19: 15–42
19. Ursino M. A mathematical study of human intracranial hydrodynamics. Part 1 – The cerebrospinal fluid pulse pressure. Ann Biomed Eng 1988, 16: 379–401
20. Drummond JC. The lower limit of autoregulation: Time to revise our thinking? (Letter) Anesthesiology 1997; 86: 1431–1433
21. Lanier WL, Albrecht RF, Iaizzo PA. Divergence of intracranial and central venous pressures in lightly anesthetized, tracheally intubated dogs that move in response to a noxious stimulus. Anesthesiology 1996; 84: 605–613